Reduction of the uncertainties in the water level-discharge relation of a 1D hydraulic model in the context of operational flood forecasting

Johan Habert, Sophie Ricci, Olivier Thual, Etienne Le Pape, Andrea Piacentini, Nicole Goutal, Mélanie, Catherine Rochoux, Gabriel Jonville

Elsevier Editorial System(tm) for Journal of Hydrology
Manuscript Draft

Manuscript Number:

Title: Reduction of the uncertainties in the water level-discharge relation of a 1D hydraulic model in the context of operational flood forecasting.

Article Type: Review Article

Keywords: Hydraulic modeling
Flood forecasting
Data assimilation
Uncertainty reduction

Corresponding Author: Mr. Johan Habert,

Corresponding Author's Institution: CERFACS

First Author: Johan Habert

Order of Authors: Johan Habert; Sophie Ricci, Senior Researcher; Olivier Thual, Professor; Etienne Le Pape, Engineer; Andrea Piacentini, Research Engineer; Nicole Goutal, Senior Researcher - Engineer; Mélanie Rochoux, Senior Researcher

Suggested Reviewers: Guy Schumann Research scientist
Hydrodynamic modeling and remote sensing of floods , JPL/UCLA, USA
guy.schumann@jpl.nasa.gov

Laura Giustarini Researcher
Institute of Science and Technology (LIST), Luxembourg
laura.giustarini@list.lu

Nelly Jean-Baptiste Hydraulic engineer
EDF, France
nelly.jean-baptiste@edf.fr

Guillaume Thirel Scientific researcher in hydrology
IRSTEA, France
guillaume.thirel@irstea.fr

Eric Gaume Deputy head of a research department
Geotechnics Water and risks, IFSTTAR
eric.gaume@ifsttar.fr

Reduction of the uncertainties in the water level-discharge relation of a 1D hydraulic model in the context of operational flood forecasting

J. Habert[a,b,*], S. Ricci[b], E. Le Pape[c], O. Thual[d], A. Piacentini[b], N. Goutal[e], M. Rochoux[b]

[a] *DREAL Champagne-Ardenne, Châlons-en-Champagne, France*
[b] *URA 1875/CERFACS, Toulouse, France*
[c] *SCHAPI, Toulouse, France*
[d] *URA 1875/CERFACS and INPT, CNRS, IMFT, Toulouse, France*
[e] *LNHE EDF-R&D, Chatou, France*

Abstract

This paper presents a data-driven hydrodynamic simulator based on the 1-D hydraulic solver dedicated to flood forecasting with lead time of an hour up to 24 hours. The goal of the study is to reduce uncertainties in the hydraulic model and thus provide more reliable simulation and forecast in real time for operational use by the national hydrometeorological flood forecasting center in France. Previous studies have shown that sequential assimilation of water level or discharge data allows to adjust the inflows to the hydraulic network resulting in a significant improvement of the discharge while leaving the water level state imperfect. Two strategies are proposed here to improve the water level-discharge relation in the model. At first, a modeling strategy consists in improving the description of the river bed geometry using topographic and bathymetric measurements. Secondly, an inverse modeling strategy proposes to locally correct friction coefficients in the river bed and the flood plain through the assimilation of in-situ water level measurements. This approach is based on an Extended Kalman filter algorithm that sequentially assimilates data to infer the upstream and lateral inflows at first and then the friction coefficients. It provides a time varying correction of the hydrological boundary conditions and hydraulic parameters.

The merits of both strategies are demonstrated on the Marne catchment in France for eight validation flood events and the January 2004 flood event is used as an illustrative example throughout the paper. The Nash-Sutcliffe criterion for water level is improved from

0.135 to 0.832 for a 12-hour forecast lead time with the data assimilation strategy. These developments have been implemented at the SAMA SPC (local flood forecasting service in the Haute-Marne French department) and used for operational forecast since 2013. They were shown to provide an efficient tool for evaluating flood risk and to improve the flood early warning system. Complementary with the deterministic forecast of the hydraulic state, an estimation of an uncertainty range is given relying on off-line and on-line diagnosis. The possibilities to further extend the control vector while limiting the computational cost and equifinality problem are finally discussed.

Keywords:

Hydraulic modeling, Flood forecasting, Data assimilation, Uncertainty reduction

---

*Corresponding author. Present address: DREAL Champagne-Ardenne/SRS/PHH/CPC, 40 boulevard Anatole France, BP80556, 51022 Châlons-en-Champagne Cedex, France. Tel:+33351416469.

Email address: johan.habert@developpement-durable.gouv.fr (J. Habert)

Contents

1. Introduction

Flooding causes important social, environmental and economic losses and is likely to be aggravated by climate change over the next decades. For example, flooding of the Var river in the South-East of France in 2010 resulted in a 700 million euros loss and 25 victims (22). Worldwide, national or international operational flood forecasting centers are in charge of providing water level predictions and flood risks at short- to medium-range lead time (from several hours to a few days) that are of great importance for civil protection. To this end, operational centers aim at providing an accurate forecast of the hydraulic variables (i.e., water level and discharge) along the monitored network. This forecast relies on the complementary use of numerical models and observations (18). For instance, the UK Environment Agency in collaboration with the Met Office has developed the National Flood Forecasting System (NFFS) in order to access to real-time forecasts from a large set of hydrologic modeling tools (38; 37). In the Philippines, the Metro Manila model is used operationally to issue 24-hour lead time forecasts using precipitation and water level measurements that are collected and transmitted in real time (20). In France, since 2006, the national and hydrometeorological flood forecasting center (SCHAPI – Service Central d'Hydrométéorologie et d'Appui à la Prévision des Inondations), in collaboration with the 22 local flood forecasting services (SPC – Service de Prévision des Crues), produces a twice-daily vigilance map available for governmental authorities and general public (http://www.vigicrues.gouv.fr). Meteorological, hydrologic and geographic data (bathymetry, topography), are used as inputs to hydraulic models that are integrated in forecast mode to describe water level and discharge at a limited number of observing stations over 22,000 km of rivers in France. These hydraulic variables are then translated into a colored flood risk map available online. On a larger scale, the European Flood Awareness System (EFAS) as part of the Copernicus Emergency Management System provides probabilistic flood alert information more than 48 hours in advance to national authorities. This alert system covers the main European rivers on a 5-km grid using a distributed hydrologic rainfall-runoff-routing model (LISFLOOD) as well as ensemble weather forecasts and real-time weather observations (8; 34).

The capacity for real-time anticipation of extreme flood events remains limited due to several sources of uncertainty in hydraulic models. On the one hand, forcing data that represent boundary conditions for hydraulic models usually result from the transformation of uncertain observed water levels into discharges with an uncertain rating curve (7; 3), or from discharges forecasted by uncertain hydrologic models. Another source of uncertainty is the description of the river channel and flood plain geometry. This requires on-site measurements of topographic and bathymetric profiles to provide a spatially-distributed geometry. On the other hand, the equations that are solved by models are based on simplification and parametrization of the physics. The parametrization schemes are calibrated to adjust the model behavior to observed water levels, typically, through the calibration of friction coefficients. The calibration of the river bed and flood plain friction coefficients is usually achieved once for all using a batch of observations such as water level from a limited number of flood events, thus providing time-invariant values for the model parameters. It is important to mention that errors in the model inputs and in the model equations are sometimes difficult to discriminate (35; 30). These uncertainties usually translate into errors in the model representation of the water level-discharge ($H - Q$) relation that is not coherent with that from the reality. In practice, this inconsistency can be reduced when complementary data become available to improve the model, for instance LIDAR data for bathymetry (horizontal resolution of one point per square meter; 10 to 30 cm of vertical accuracy). When no additional data are available to improve the model geometry, the error between the simulated and the observed hydraulic states must be accounted for by adjusting the model parameters and/or the model state itself. Many studies have attempted to account for uncertainties at varying levels (36; 19), for instance by analyzing the uncertainty in hydrologic prediction based on the Generalized Likelihood Uncertainty Estimation (GLUE) (5; 2; 25; 33), Markov chain Monte Carlo (MCMC) (16), Bayesian inference (27) and Data Assimilation (DA) (19; 24; 10; 9).

DA offers a convenient and cost-effective framework, compared to MCMC and Bayesian inference, to overcome some limits of the classical calibration process for model parameters: observations and simulation outputs are combined along with their respective errors to

estimate an optimal set of model parameters and thereby reduce simulation uncertainties. Furthermore, as the DA algorithm is sequentially applied, the analysis allows for a temporal variation of model parameters errors. The classical approach in DA for meteorology and oceanography is to directly correct the model output variables (also called state estimation). In the hydrology and hydraulic literature, the estimation of uncertainty in model parameters has been extensively investigated in addition to the more traditional state estimation approach. Sequential state estimation for hydraulic applications was indeed found to have a limited impact on the forecast performance due to the limited persistence of the model initial condition. In contrast, the forecast lead time can be significantly improved via the correction of the hydrologic forcing (14; 1; 31) or of the model parameters (11). Through the inclusion of parameters in the DA process, it is assumed that the forecast uncertainty can be efficiently reduced over a time window for which the errors statistics in the model parameters are stationary. State and parameter correction can be performed independently, or simultaneously (24; 23) with an augmented state as illustrated in (15). For example, (26) focused on state estimation and assimilated water level observation derived from spaceborne imaging and digital terrain model to estimate discharge in an un-gauged basin simulated by a coupled hydrologic and hydrodynamic model. (14) and (21) used ensemble-based approaches (the Ensemble Kalman Filter – EnKF – and particle filters, respectively) to update the state but also to infer the upstream boundary conditions. (4) explored the assimilation of hydrologic data into operational hydrologic forecast to correct several input parameters including river bed friction coefficients.

The present study illustrates how errors in the water level-discharge relation of a 1D hydraulic model can be accounted for in the context of operational flood forecasting following two different approaches. The first method is based on the assumption that additional data on the river bed geometry are available to directly improve the model $H - Q$ relation. In the following, this approach is referred to as experiment BATHY. For the second method, it is assumed that the only additional data available are in-situ water level measurements, which are used in real time to adjust the river bed and flood plain friction coefficients in the model using a DA algorithm. In the following, this approach is referred to as experiment

ASSIM. A time-dependent correction of the friction coefficients is provided by DA in order to account for errors in the friction and bathymetry description that vary along with the flow as water level reaches different portions of the described geometry. It should be noted that the errors in the model $H - Q$ relation are potentially larger at high flow since the flood plain topography is not well known and since the model is not well calibrated. Thus, this study aims at demonstrating that both approaches BATHY and ASSIM can significantly improve the model $H - Q$ relation and subsequently the simulated hydraulic state. This work is carried out in the context of operational flood forecasting at the SAMA (Seine Amont Marne Amont) SPC for the Marne catchment in France. SAMA uses the 1D hydraulic model MASCARET (12) developed by LNHE (Laboratoire National d'Hydraulique et d'Environnement) from EDF-R&D (Electricité De France – Recherche et Développement) to simulate real-time discharge or water level forecasts at six observing stations on the upstream part of the Marne river. Maximum forecast lead time for each site is between 5 and 21 hours according to the transfer time along the hydraulic network. The reference model for this work, referred to as experiment REF in the following, results from a classical batch calibration procedure of the un-gauged upstream and lateral inflows to the model as well as of the river bed and flood plain friction coefficients. In this context, (31) demonstrated that the assimilation, based on an Extended Kalman Filter (EKF) algorithm, of water level observations to correct hydrologic boundary conditions and hydraulic model parameters on the Adour catchment with MASCARET improves flood forecasting by 60 % for 1-hour lead time and by 25 % for 12-hour lead time. A similar approach using discharge data was then applied to the Marne catchment to specify upstream and lateral inflows (13), resulting in the significant improvement of the simulated discharge state, while the simulated water level state remained imperfect. The correction of un-gauged lateral and upstream inflows with DA offers an alternative solution to the classical batch calibration procedure by considering a time-varying estimation of the boundary conditions. In the present work, this corresponds to the first step of the DA method referred to as experiment ASSIM1 in the following. Further improvement on the river bed and flood plain friction coefficients in the neighborhood of the observing stations is obtained with water level assimilation. This represents the second

step of the DA method referred to as experiment ASSIM2 in the following. The method ASSIM is therefore a two-step DA procedure: ASSIM1 allows for the correction of upstream and lateral inflows and ASSIM2 allows for the correction of river bed and flood plain friction coefficients. The sequential application of both steps in ASSIM is referred to as experiment ASSIM1+ASSIM2.

The structure of the paper is as follows: Section 2 provides a description of the Marne catchment and of the materials (hydraulic model, DA method) used to perform flood forecasting. The evaluation of the linearity of the water level with respect to the friction coefficients is investigated. The limitations of the reference model REF are highlighted and the two-step DA strategy ASSIM is presented in detail. In Sect. 3, the results of both BATHY and ASSIM approaches are presented using the January 2004 flood event as an illustrative example. The operational implementation of the ASSIM approach at the SAMA SPC is described in Sect. 4. Conclusions and perspectives for this work are given in Sect. 5.

2. Materials and methods

2.1. The 1D hydraulic model MASCARET

The Marne river is an important tributary of the Seine river in France. Its source is located on the Langres plateau in the Haute-Marne department. A mono-dimensional hydraulic model is used to simulate the hydrodynamics of the 180-km Marne river as presented in Figure 1. This study is carried out in the upstream part of the Marne river where flash floods frequently occur; for instance, in December 2011, the discharge at Condes raised from 25 to 125 m^3/s in 24 hours. Upstream boundary conditions (black dots in Figure 1) for the hydraulic network are described with observed water levels that are translated into discharges with a local rating curve; the downstream boundary condition at Chamouilley is also described with a local rating curve. There are six observing stations located on the main stream of the river (black triangles in Figure 1) where water level is measured hourly. These data are provided by the DREAL (Direction Régionale de l'Environnement, de l'Aménagement et du Logement) hydrometeorological service in the Champagne-Ardenne region.

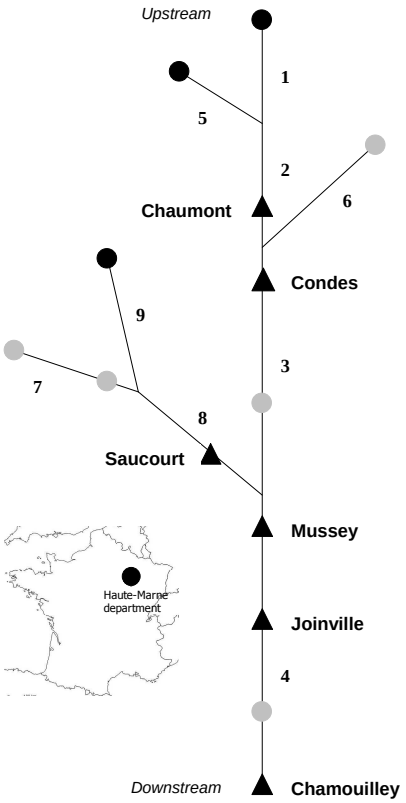

Figure 1: Schematic of the Marne model hydraulic network (Haute-Marne, France). Observed upstream flows are represented with black dots; additional inflows are represented with grey dots; and observing stations over the hydraulic network are represented with triangles.

Along this hydraulic network, the 1D form of the Saint-Venant equations is solved with the MASCARET (12) software developed by EDF-R&D and CEREMA (Centre d'Etudes et d'Expertise sur les Risques, l'Environnement, la Mobilité et l'Aménagement), widely used for modeling flood events, submersion waves resulting from the failure of hydraulic infrastructures, river control, and channel waves propagation. The 1D Saint-Venant equations read (non-conservative form):

$$\frac{\partial S}{\partial t} + \frac{\partial Q}{\partial x} = q_a \quad , \quad \frac{\partial Q}{\partial t} + \frac{\partial QV}{\partial x} + gS(\frac{\partial Z}{\partial x} + J + J_s) = 0 \; with \; J = \frac{Q^2}{S^2 K_s^2 R_H^{4/3}}. \qquad (1)$$

where S [m^2] is the river section, Q [m^3/s] is the discharge, q_a(x,t) is the lateral lineic

discharge, K_s [$m^{1/3}.s^{-1}$] is the friction coefficient, R_H is the hydraulic radius, g is the gravity, J and J_s represents regular and singular head losses respectively. The river section S is, for each location x, a function of the water level $H = Z(x,t) - Z_{bottom}(x,t)$, where $Z(x,t)$ [m] is the free surface height and where Z_{bottom} [m] corresponds to the river bed bathymetry. The unsteady kernel of MASCARET was used in this study.

The Marne terrain model was built with 110 topographic and bathymetric cross sections; it was calibrated in 2011 using a batch of water level and discharge measurements from ten flood events at Chaumont, Condes, Saucourt, Mussey, Joinville and Chamouilley. The model was then validated over eight independent flood events that occurred between 2004 and 2013; these events can be classified in three types: two events with a maximum discharge of 100 m^3/s at Mussey, two events with a maximum discharge at Mussey ranging between 115 and 240 m^3/s, and three stronger events with a maximum discharge at Mussey above 260 m^3/s (among which the January 2004 flood event used in this paper for illustrative purposes). Five upstream and lateral inflows (grey dots in Figure 1) were added to the model to represent additional water input to the network. At these five locations, despite the lack of hydrologic rainfall-runoff model, the hydrograph is described as proportional to a mean upstream area hydrograph; the multiplicative coefficients used for the model in the present work were optimized by a batch calibration procedure. Additionally, the river bed and flood plain friction coefficients (denoted respectively by m and n) were calibrated by minimizing simulated and observed discharge differences; the resulting calibrated friction coefficients that have a straightforward influence on the $H - Q$ relation in the model are given in Table 1. In the following, the model with batch calibration corresponds to the reference model denoted by REF.

The Nash-Sutcliffe criteria for water level N_H and discharge N_Q were calculated for the eight validation flood events for each observing station using the following formulation given

for Q:

$$N = 1 - \frac{\sum_{i=1}^{n}(Q_i^{obs} - Q_i^{sim})^2}{\sum_{i=1}^{n}(Q_i^{obs} - \overline{Q}^{obs})^2}, \tag{2}$$

where Q_i^{obs} and Q_i^{sim} correspond to the observed and simulated discharges at time indexed by i, and where $\overline{Q}^{obs}$ denotes the time-averaged value of the observed discharges. The Nash-Sutcliffe criteria results are presented in Table 1. In general, the quality of the results decreases from upstream to downstream as the use of mean multiplicative coefficients generates errors in the lateral and upstream inflows estimation. Additionally, the Nash-Sutcliffe criteria computed with respect to discharge Q are generally better than when computed with respect to water level H, especially at Mussey (Reach 4, Portion 1 in Table 1). It should be noted that there is no rating curve available at Joinville, thus no discharge data at this observing station. For the January 2004 flood event used in this work for illustrative purposes, the Nash-Sutcliffe criteria associated with the REF model and presented in Table 2 are respectively 0.773 and 0.894 for water level and discharge. The criteria are here computed in re-analysis mode that corresponds to a 0-h forecast lead time (details are given in Sect. 2.2). REF (dashed lines) and observed (dotted lines) hydraulic states at Mussey are compared in Figure 2 over the January 2004 flood event (thin lines correspond to water level, thick lines correspond to discharges). The difference between REF and observations varies over time for both water level and discharge, thus arguing for a time-dependent correction as enabled by DA in Sect. 2.2. It is important to notice that the sign of the error in discharge and in water level are different for high flow conditions (flood peak from day 4 to day 5), while similar away from the flood peak. For high water levels, the discharge is slightly overestimated (by 25 m^3/s at day 5), whereas the water level is significantly underestimated (by 0.4 m at day 5). During this period, the $H - Q$ relation in the model is incorrect, a negative correction in the discharge would further deteriorate the water level state. Thus, for this event, the batch calibration process is to fail at providing parameters (friction coefficients and upstream/lateral inflows) that would improve both discharge and

water level at the flood peak (the same assumption seems legitimate at Joinville). It is then obvious that the reference model (REF) should be improved as explained in the following.

Reaches	**Portions**	**Length**	**m**	**n**	**Observing stations**	N_H	N_Q
1	1	5,172	24	14			
2	1	21,753	24	14	Chaumont	0.922	
3	1	660	36	22	Condes	0.821	0.835
	2	44,842	24	14			
4	1	578	20	13	Mussey	0.544	0.743
	2	8,200	24	18			
	3	300	14	8	Joinville	0.531	
	4	26,383	24	14	Chamouilley	0.614	0.621
5	1	4,150	24	14			
6	1	27,101	24	14			
7	1	7,600	9	7			
8	1	16,266	9	7			
	2	500	13	8	Saucourt	0.797	0.821
	3	5,680	9	7			
9	1	10,819	9	7			

Table 1: Mean friction coefficients obtained after calibration for the river bed (m) and the flood plain (n) in [$m^{1/3}.s^{-1}$], as well as Nash criteria for water level (N_H) and discharge (N_Q) calculated for eight validation flood events and for reaches 1 to 9 over the Marne model hydraulic network. Reaches lenghts are in meters.

2.2. Sequential DA method

2.2.1. DA algorithm

The DA method (ASSIM) is a two-step procedure using an EKF algorithm.

The first step ASSIM1 consists in correcting the upstream and lateral inflows to the model using discharge data, with the objective to improve the simulated discharge. The

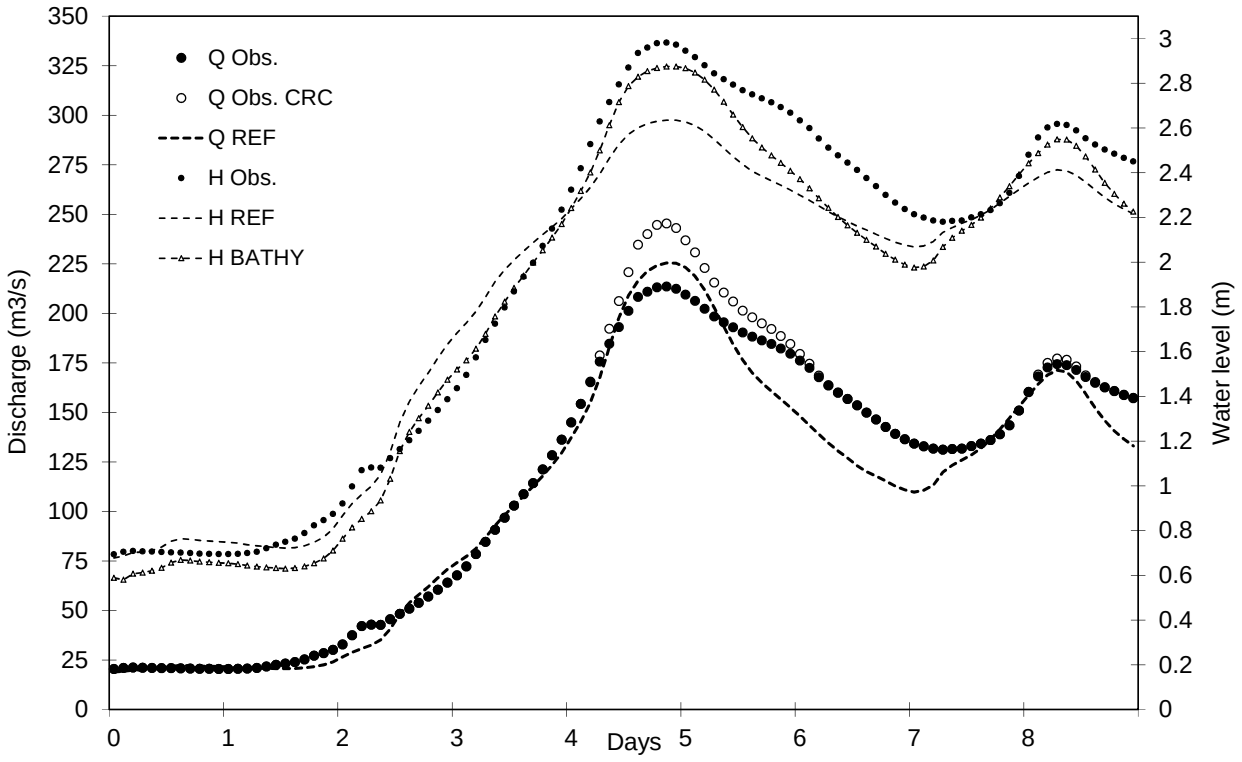

Figure 2: Simulated water levels (thin lines) and discharges (thick lines) at Mussey for REF (dashed line) and BATHY (dashed line with triangle – discharges are unchanged) for the January 2004 flood event. Observations are represented with small and large black dots for water level and discharge, respectively. Circles represent the discharge observations obtained with the Corrected Rating Curve (CRC).

ASSIM1 method is presented in details in (31) and (13). For the Marne applicative test case, discharge observations (Condes, Mussey, Chamouilley and Saucourt) are assimilated to correct the five upstream and lateral inflows along the hydraulic network (represented by grey dots in Figure 1) in order to correctly represent discharge.

In spite of the discharge improvement, when the model $H - Q$ relation is incorrect (at high flow), the simulated water level remains imperfect. These errors are here accounted for in the second step ASSIM2, which uses water level data to locally correct river bed and flood plain friction coefficients in the neighborhood of the observing stations. The batch calibration process leads to an estimate that allows, on average, the model to correctly

	N_H	N_Q
REF	0.773	0.894
BATHY	0.923	0.897
ASSIM1	0.784	0.976
BATHY+ASSIM1	0.986	0.987
ASSIM1+ASSIM2	0.97	0.978

Table 2: Nash-Sutcliffe criteria for REF, BATHY, ASSIM1 and ASSIM1+ASSIM2 experiments for water level (N_H) and discharge (N_Q) in re-analysis mode for the January 2004 flood event at Mussey.

simulate a set of flood events. Depending on the choice of this set of events, the calibrated friction coefficients might be better fitted for low, medium or high flow. Usually, high flow are not well represented. It thus makes sense to look for a time-varying correction of the friction coefficients during a flood event. Additionnaly, the bathymetry is described from a limited number of measured cross sections. The correction of the friction coefficients offers a way to also account for the uncertainty related to bathymetry. In the present study, the friction coefficients are corrected over a 600-m section in the vicinity of the observing station at Mussey (Portion 1 of reach 4) and over a 300-m section in the vicinity of Joinville (Portion 3 of reach 4). These coefficients were chosen as their uncertainty has a significant influence on the simulated water level at the observing stations; still the following method could be applied to any friction coefficient for the hydraulic network. The friction coefficients in the river bed and in the flood plains, respectively denoted by m and n, are gathered in the control vector $\mathbf{x}$ of size $s = 4$ in the present case study. The background values in $\mathbf{x}^b$ are those specified from the calibration procedure ($m^b = 20$ and $n^b = 13$ for Mussey; $m^b = 14$ and $n^b = 8$ for Joinville). The errors in m and n are supposed to be uncorrelated, and the respective standard deviation (STD) are set according to the variability in the calibration procedure ($\sigma_m^b = 3$ and $\sigma_n^b = 4$ at Mussey; $\sigma_m^b = 3$ and $\sigma_n^b = 2$ at Joinville). Hourly water level observations are assimilated over a time window at Mussey and Joinville and gathered in the observation vector $\mathbf{y}^o$ of size p. The errors in the water level observations are supposed

to be uncorrelated; the observation error STD σ_o is set to 0.025 m to account for errors in the adjustment of the measurement pressure tube.

Following the classical equations of the Kalman filter (17), the analysis vector $\mathbf{x}_k^a$ for cycle k can be formulated as a correction to the background vector $\mathbf{x}_k^b$ as follows:

$$\mathbf{x}_k^a = \mathbf{x}_k^b + \mathbf{K}_k\Big(\mathbf{y}_k^o - H_k(\mathbf{x}_k^b)\Big), \tag{3}$$

where $\mathbf{K}_k = \mathbf{B}_k\mathbf{H}_k^T\left(\mathbf{H}_k\mathbf{B}_k\mathbf{H}_k^T + \mathbf{R}_k\right)^{-1}$ is the gain matrix, $\mathbf{B}_k$ and $\mathbf{R}_k$ are respectively the background and observation errors covariance matrices, and $\mathbf{H}_k$ is the Jacobian of H_k at $\mathbf{x}_k^b$. The analysis error covariance matrice is:

$$\mathbf{A}_k = (\mathbf{I} - \mathbf{K}_k\mathbf{H}_k)\,\mathbf{B}_k. \tag{4}$$

The generalized observation operator H_k is used to describe the model counterpart of the observations $\mathbf{y}_k^o = H_k(\mathbf{x}_k)$ associated with the control vector $\mathbf{x}_k$. It consists in, first integrating the hydraulic model using the friction coefficients in $\mathbf{x}^b$, then selecting the corresponding simulated water level at the observed point and time. This operator is non-linear with respect to $\mathbf{x}$ as it implies the integration of the hydraulic model; this issue will be further investigated in Sect. 2.2.2 as it is a limiting point for the EKF algorithm optimality. The Jacobian $\mathbf{H}_k$ of the observation operator H_k is a $s \times p$ matrix: each column represents the variation in the hydraulic variables at the observing locations and times that are due to the perturbation of an element of the control vector (corresponding to one friction coefficient over a given location). In the present work, it is conveniently computed in the vicinity of the background vector at the analysis time k with a finite difference scheme that requires additional hydraulic model integrations; these independent integrations are run in parallel using the Parasol functionality of the OpenPALM dynamic coupler (6), a framework that is convenient to develop DA methods in a modular way. The Jacobian matrix is computed for each analysis cycle as the impact of a perturbation in the friction coefficients on the hydraulic variables depends on the hydraulic state itself.

Since there is no explicit propagation model for parameters (29; 24; 28; 32), the usual propagation steps of the KF algorithm are irrelevant here; a persistence model is often

assumed for the parameters between the analysis cycles. In the present implementation, the background vector $\mathbf{x}_k^b$ and the background error covariance matrix $\mathbf{B}_k$ are kept invariant between the cycles (for every cycle k). For that reason, the present EKF algorithm can be considered as an invariant EKF (relatively to the background information). It is worth noting that for a given cycle, the initial condition for the background simulation is derived from the analysis simulation obtained during the previous cycle; consequently, each cycle restarts with an improved initial condition. Thus, the background 78-hour run differs from the corresponding portion (in time) of the continuous reference run (REF) since both runs start from a different model state at the cycle initial time. It is also worth mentioning that advanced pseudo-model for parameters could be implemented; this question will be addressed in further work. The small size of the control vector (less than 10 for the Marne test case) enables the use of an EKF algorithm, involving matrix operations for the computation of the gain matrix along with a finite difference scheme for the computation of the generalized observation operator Jacobian.

The cycling of the analysis is presented in Figure 3 for ASSIM1 and in Figure 4 for ASSIM2 following ASSIM1. The assimilation is performed over a cycle k of 66 hours with 54 hours of re-analysis and 12 hours of forecast at Mussey. The forecast period is adjusted for each observing station and decreases going downstream. Over the 54-hour re-analysis period, the hydrologic upstream and lateral forcings are supposed to be known (either observed or calibrated). Over the forecast period, the forcings are supposed to be unknown and set constant to the last known value. The 54-hour re-analysis period corresponds to a 48-hour period over which the model adjusts to the initial state, plus a 6-hour period over which observations are assimilated using the EKF algorithm. Hence, the size of the observation vector in the present study is $p = 12$. The last observation time from which the forecast integration starts is the analysis time T. For cycle k, in ASSIM1 (Figure 3), over the 6-hour assimilation period (hatching area), the background issued from the previous analysis cycle (solid line) and observed discharges (black dots) are compared and a correction to the inflows is obtained through the EKF analysis step. The correction is applied over the re-analysis and the forecast periods, thus assuming that the nature of the errors in the upstream and

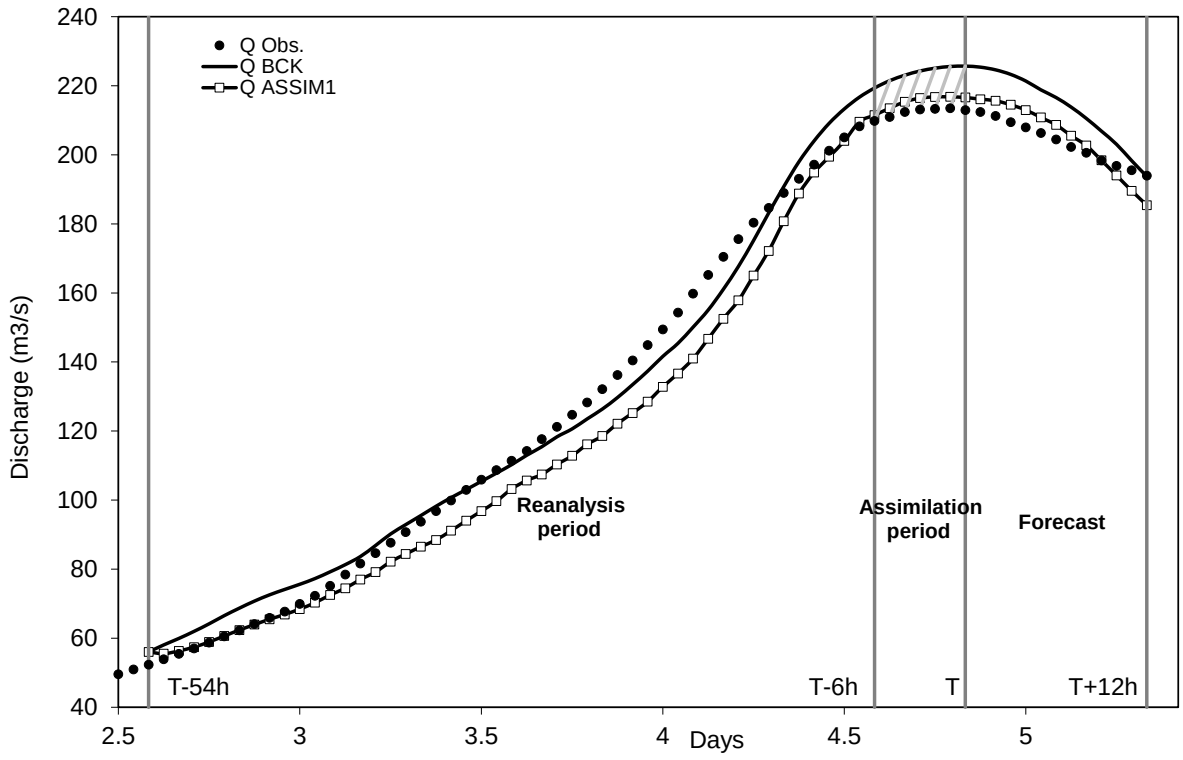

Figure 3: Observed (black dots), background from previous cycle (BCK solid line) and analyzed discharges (squared solid line) for the ASSIM1 approach at the flood peak at Mussey for the January 2004 flood event for T = 417,600 s = 4.83 days.

lateral inflows remains the same over the forecast period. The analyzed forcings are used to achieve a new model integration (over the 66-hour time period), which provides a better discharge state, while the water level can be either improved or degraded depending on the coherence between the model and the observation $H - Q$ relation.

The analyzed water level from ASSIM1 is then used as the background state for ASSIM2; it is compared to water level observations over the 6-hour assimilation period and the EKF update provides a correction to the river bed and flood plain friction coefficients m and n, which results in the water level improvement as shown in Figure 4 (squared solid line). The oscillations at the beginning of the cycle are due to the inconsistency between the initial state (stored from a previous cycle analysis) and the friction coefficients for the current cycle. The assimilation window is shifted hourly and the sequential application of ASSIM1+ASSIM2

provides a corrected hydraulic state and forecast. This cycled DA procedure allows for a temporal variability of the friction coefficients over a flood event, which can be either associated to real changes in the river bed and flood plain friction or geometry properties as well as to various types of errors that are artificially accounted for here by correcting m and n.

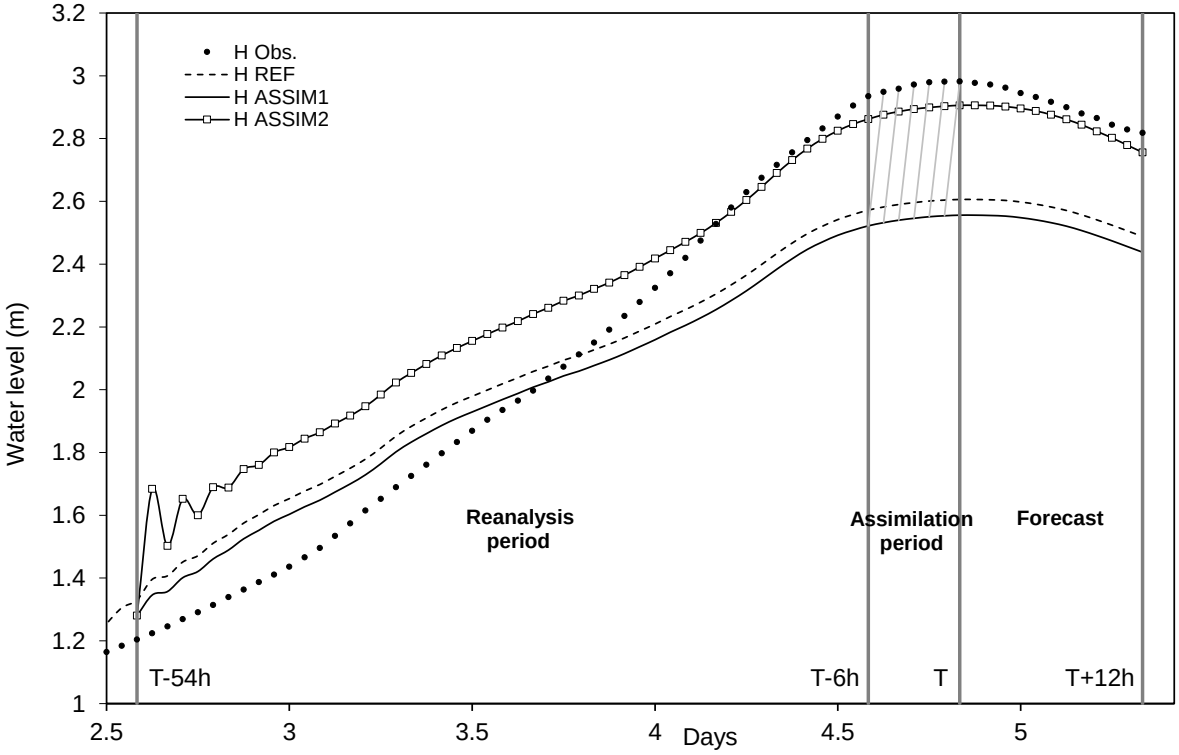

Figure 4: Observed (black dots), background from ASSIM1 (solid line) and analyzed (squared soline line) water levels for the ASSIM2 (following ASSIM1) approach at the flood peak at Mussey for the January 2004 flood event for T = 417,600 s = 4.83 days. Water level from ASSIM1 used as the background state for ASSIM2 is compared to water level observations to provide analyzed friction coefficients and subsequently, corrected water level.

2.2.2. Study on the linear assumption of the generalized observation operator

The EKF algorithm relies on the hypothesis that the generalized observation operator can be approximated by a linear operator on the $[\mathbf{x}^b, \mathbf{x}^a]$ interval. The linearity of the hydraulic model response to a perturbation in the river bed and flood plain friction coefficients m and n was thus investigated. Figure 5 presents the probability density function (pdf) of the simulated water level at Mussey for a permanent flow ($Q = 150$ m^3/s) when the friction coefficient at Mussey for the minor bed is perturbed around the background mean value $m = 20$. The 10,000 perturbations are randomly chosen following a Gaussian function with a variance of 12.

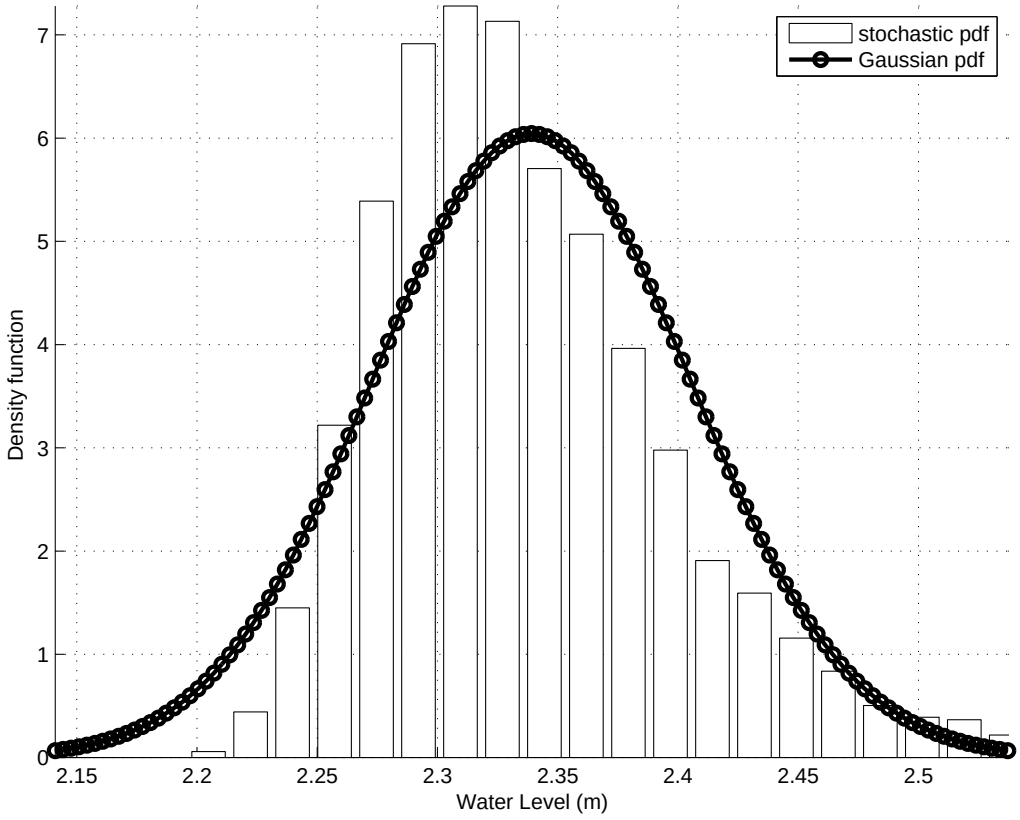

Figure 5: Water level pdf for 10,000 perturbations of the river bed friction coefficient m with a variance of 12. The solid line represents the analytical pdf corresponding to a Gaussian model response; and the histogram represents the actual MASCARET hydraulic model response reconstructed from the 10,000 model outputs.

In Figure 5, the pdf in solid line is a Gaussian function built from the first two moments (mean and variance) of the system response assuming a linear relation in the model. The actual response is represented by the shaded histogram that is obviously non-symmetrical. First, there is a larger amount of water-level values that are smaller than the mean of the Gaussian pdf. This means that the (negative) water level anomaly resulting from a small positive perturbation δm of the friction coefficient is bigger than the (positive) water level anomaly resulting from a negative perturbation $-\delta m$ of the friction coefficient. Secondly, the stochastic pdf is amplified for extreme water level values, meaning that a large (negative) perturbation of the friction coefficient m results into a large (positive) perturbation of the water level when a large (positive) perturbation of the friction coefficient has a smaller impact. The same test was carried out with n; similar conclusions were drawn. It was also found that the impact of a perturbation of m and n increases when the discharge increases. Figure 6 assesses the impact of a perturbation δn (where $x^{\mathrm{b}} = 13$) between –12 and 12 on the simulated water level at Mussey for different discharges. A perturbation of -6 for n leads to a variation of 0.01 m when $Q = 80$ m^3/s and to a variation of 0.03 m when $Q = 225$ m^3/s.

Based on these results, it is assumed in the following that the relation between the friction coefficients and the hydraulic state is reasonably approximated by a linear function in the vicinity of $\mathbf{x^b}$. The Jacobian matrix of the generalized observation operator $\mathbf{H}_k$ is computed around the background values for m and n for a perturbation $\delta m = -2$ and $\delta n = -1$ using a finite differences scheme in consistency with the linearity study. In order to avoid non-physical values for the friction coefficients as well as to limit the nonlinear impact, minimum and maximum threshold values are applied to the friction coefficients with [14, 24] for m and [8, 20] for n.

3. Correction of the model $H - Q$ relation

3.1. Bathymetric profiles densification (BATHY)

This section presents the method for experiment BATHY; it is assumed that the $H - Q$ relation in the 1D hydraulic model is improved by adding geometric data to the model.

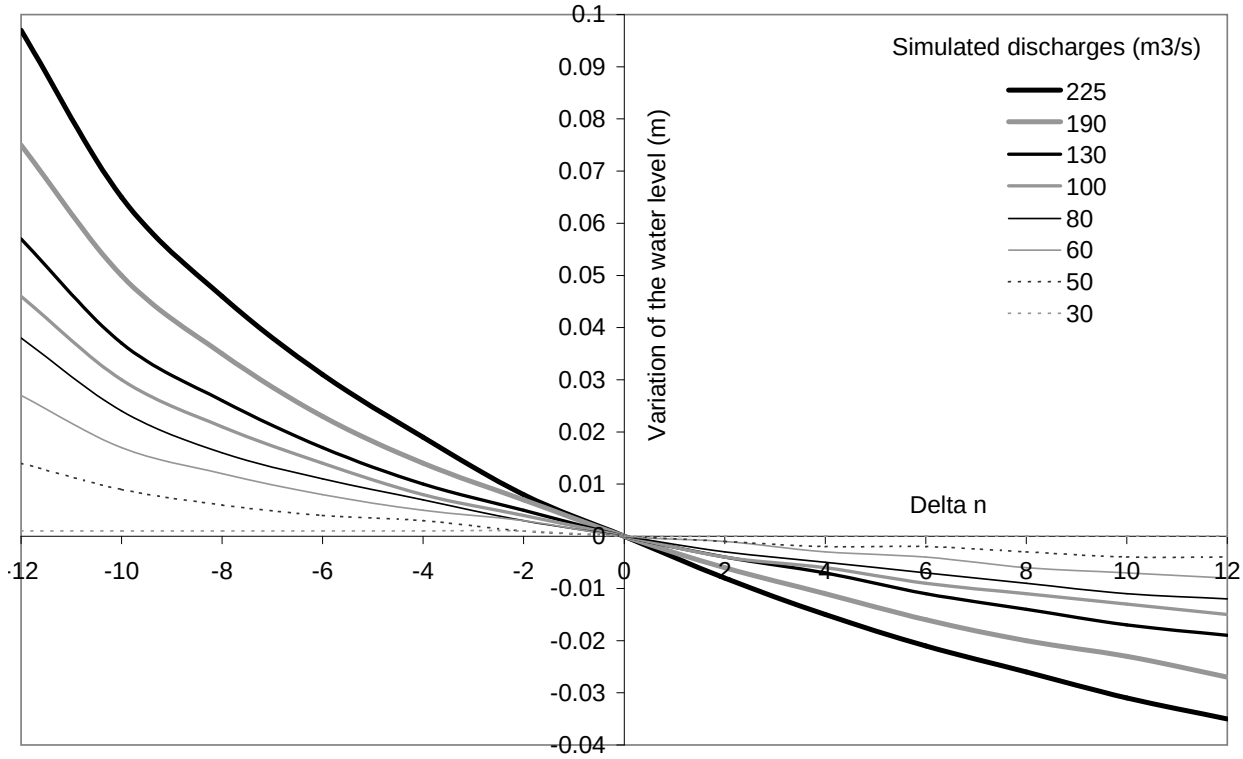

Figure 6: Impact of the flood plain friction coefficient perturbations δn on the water level [m] for different simulated discharges [m^3/s]. A -10 and +10 perturbation of n generates a non equivalent variation of the water level but for low perturbations, the relation between friction coefficients and water level can be considered as linear.

Additional measurements of the river bed and flood plain geometry were made available near Mussey: 4 topographic and bathymetric measurements were performed in the surrounding of the observing station. The batch calibration of the local friction coefficients was then re-processed on sections 1 and 2 for reach 4. The friction coefficients for these two sections were set to $m = 30$ and $n = 8$. Figure 2 illustrates the positive impact of the cross-section densification for the January 2004 flood event for water level (dashed line with triangles). As presented in Table 2, for experiment BATHY, the Nash-Sutcliffe criterion for H is improved from 0.773 to 0.923, even though a 10-cm underestimation remains. The discharge results are left unchanged by this local bathymetry correction with a 0.897-Nash-Sutcliffe coefficient for BATHY (compared to 0.894 for REF); a small overestimation at the flood peak remains

(10 m^3/s) for this event. As shown in Table 3, the Nash-Sutcliffe criteria values computed for water level over the eight validation flood events in re-analysis mode for BATHY are better than those computed for REF, especially at Mussey where the additional geometry measurements were made; in contrast, the impact at Joinville is small.

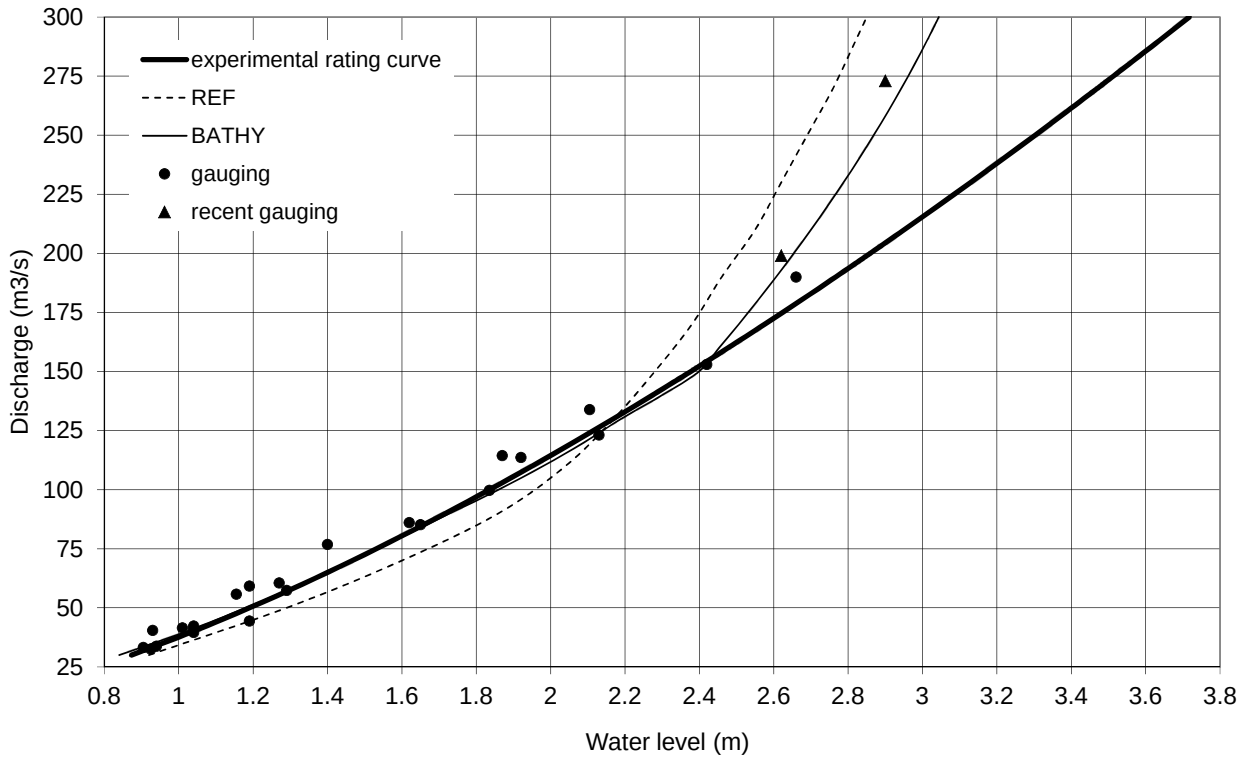

Figure 7: Comparison of the $H - Q$ relation at Mussey, derived experimentally (thick solid line) from gauging (black dots/triangles), involved in the reference model REF (thin dashed line) and obtained through the BATHY approach (thin solid line). Recent gaugings are represented with black triangles.

In Figure 7 the $H - Q$ relation for REF is represented by the thin dashed line, and the $H - Q$ relation for BATHY is represented by a thin solid line. It is shown that the BATHY $H - Q$ relation is in better agreement with all available gauging (black dots and triangles) than the REF $H - Q$ relation. As a consequence, the new model $H - Q$ relation should be used to produce discharge data from water level measurements at Mussey, in place of the experimental rating curve (thick solid line) that is in good agreement with low

Observing stations	Mussey		Joinville
	N_H	N_Q	N_H
Forecast lead time	0h	0h	0h
REF	0.601	0.722	0.653
BATHY	0.681	0.721	0.661
ASSIM1	0.754	0.854	0.779
BATHY+ASSIM1	0.858	0.853	0.784
ASSIM1+ASSIM2	0.859	0.842	0.992
Forecast lead time	12h	12h	12h
REF	0.135	0.238	0.154
BATHY	0.272	0.241	0.158
ASSIM1	0.689	0.807	0.695
BATHY+ASSIM1	0.781	0.802	0.698
ASSIM1+ASSIM2	0.832	0.807	0.907

Table 3: Nash-Sutcliffe criteria for REF, BATHY, ASSIM1, ASSIM1+ASSIM2 and BATHY+ASSIM1 computed over eight flood events for 2004-2013 at maximum lead time (12 hours) at Mussey and Joinville.

flow measurements but can lead to an underestimation of up to 60 m^3/s for high flow. It should be noted that the experimental rating curve was built from numerous gaugings below 150 m^3/s (black open dots) and only two gaugings above 150 m^3/s. Additionally, two recent gaugings for high flow (black triangles) allow to validate the BATHY model $H - Q$ relation over the entire range of discharge values at the observing station. Figure 2 presents the corrected observed discharges that are derived from water level measurements at Mussey using the BATHY densified model $H - Q$ relation (black circles). Using these corrected measurements, the model now slightly underestimates both water level (thin dashed line) and discharge (thick dashed line) at the flood peak. The sign of the errors in discharge and water level are now the same over the entire flood event, meaning that the optimization of upstream and lateral inflows as proposed in (13) is an appropriate solution for further flood

forecast improvement for both discharge and water level states.

3.2. Data assimilation for friction coefficients correction (ASSIM)

In this section, it is assumed that no additional geometric measurement is available. The reference model $H - Q$ relation is improved accounting for errors in friction coefficients and by artificially accounting for local bathymetry error with the sequential estimation of the river bed and flood plain friction coefficients m and n in the surrounding of the observing stations at Mussey and Joinville (experiment ASSIM).

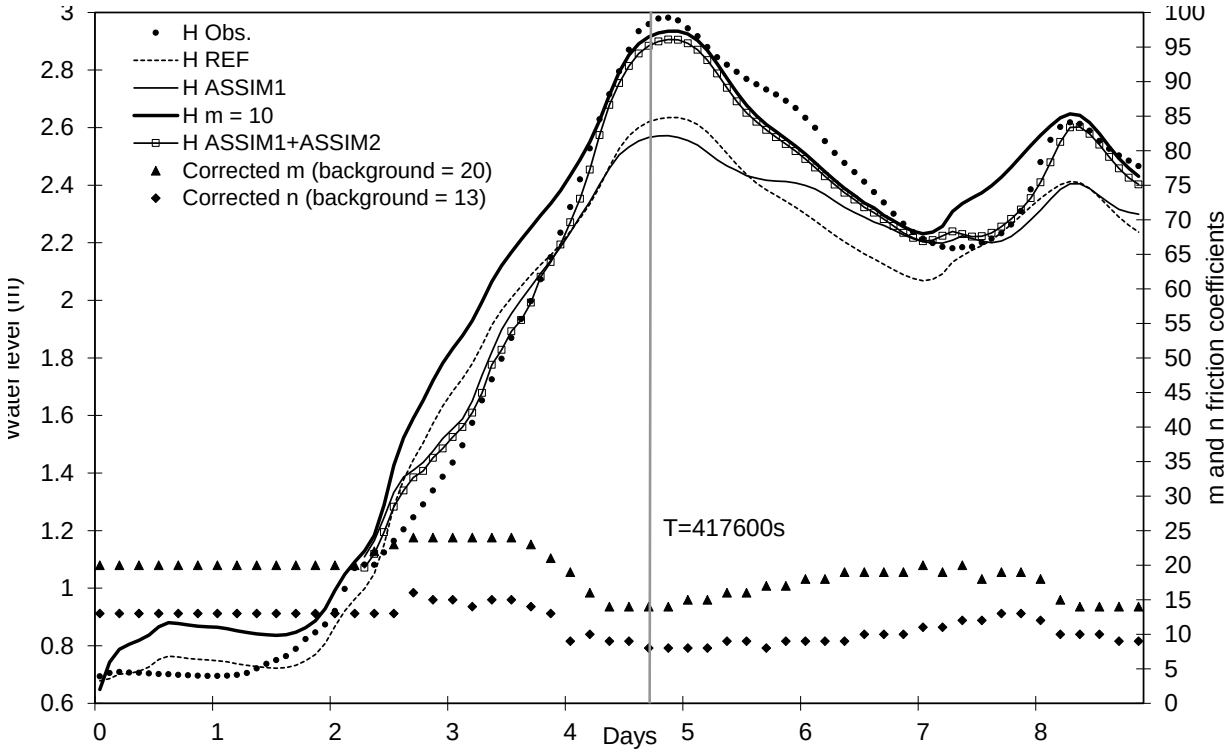

Figure 8: Observed water levels, REF (dashed line), model with $m = 10$ (thick solid line), background from ASSIM1 (thin solid line), ASSIM1+ASSIM2 (squared solid line) for the January 2004 flood event at Mussey. Corrected friction coefficients for river bed (m) and flood plain (n) from DA analysis are represented with triangles and diamonds respectively.

Figure 8 illustrates that the water level can be efficiently increased at Mussey, compared to that of REF ($m = 20$ and $n = 13$ represented with a thin dashed line), when decreasing the

river bed friction coefficient to $m = 10$ (thick solid line), while discharges are left unchanged (not shown). The value $m = 10$ is appropriate for high flow but leads to a water level overestimation for low flow condition. The friction coefficient estimation should then be flow dependent and provide time-dependent friction coefficients that account for varying errors in the friction and bathymetry river bed as the flow occupies a varying portion of the river and the flood plain. For this purpose, the DA method ASSIM detailed in Sect. 2.2 is cycled over the entire flood event to estimate upstream and lateral inflows (ASSIM1), and river and flood plain friction coefficients (ASSIM2) over time using hourly observed discharge and water level at Mussey. Corrected lateral and upstream forcings from ASSIM1 are used to provide the background state (thin solid line) for the friction coefficient estimation in ASSIM2. It should be noted that while ASSIM1 leads to a significant correction of discharge, the water level in ASSIM1 remains close to that of REF. The ASSIM1+ASSIM2 DA analysis for water level is presented for time T from day 2.25 to the end of the flood event in Figure 8 (squared line). For instance, at day 3, REF overestimates the water level, ASSIM1+ASSIM2 increases the friction coefficients in order to decrease the simulated water level. On the contrary, over the flood peak period (days 4-7), REF underestimates the water level, ASSIM1+ASSIM2 decreases the friction coefficients in order to increase the simulated water level.

The Nash-Sutcliffe criteria for water level and discharge computed at Mussey for January 2004 in re-analysis mode are presented in Table 2. ASSIM1 improves the discharge Nash value from 0.894 (REF) to 0.976; it is not significantly affected by ASSIM2 (0.978). The water level Nash value is not significantly modified by ASSIM1 (0.773 for REF compared to 0.784 for ASSIM1); it should be noted that ASSIM1 can either lead to an improvement or a degradation of the water level (as it is the case at the flood peak). However, it is greatly improved with ASSIM2 to 0.97. These results are also obtained over the eight validation flood events: the Nash-Sutcliffe criteria computed at Mussey and Joinville in re-analysis mode (0-hour forecast lead time) as well as at the maximum lead time forecast (12 hours) are presented in Table 3 for REF, BATHY and ASSIM. In re-analysis mode, ASSIM1 greatly improves the discharge results, while ASSIM2 provides improved water level states at Mussey and Joinville since the friction coefficients are corrected in the vicinity of both observing

stations. In forecast mode, the upstream and lateral hydrologic forcings are supposed to be unknown and set constant to the last observed value. As a consequence, the Nash-Sutcliffe coefficients for REF and BATHY decrease as the forecast lead time increases. The correction of upstream and lateral inflows from ASSIM1 enables a correction of the forcing over the forecast period, thus allowing for a significant improvement of the results at a 12-hour forecast lead time. The water level Nash criteria is further improved by ASSIM2 for Mussey and Joinville. For ASSIM1 and ASSIM2, it is assumed that the correction computed over the analysis period can be applied over the forecast period; as the nature of the errors varies in time, this assumption is less and less valid as the forecast lead time increases and the merits of ASSIM decrease.

It should be noted that the local densification of the geometric description (BATHY) when applied sequentially with ASSIM1, leads to similar results to ASSIM1+ASSIM2 at Mussey but not at Joinville, where no additional bathymetric measurements were available. ASSIM thus appears as an efficient approach for improving and forecasting both discharge and water level given no additional data on the river bed and flood plain geometry. Following these tests, the approach ASSIM1+ASSIM2 has become recently operational at SPC SAMA: the assimilation of discharge measurements used in real-time mode to better quantify upstream and lateral inflows (ASSIM1) has successfully run since December 2013; the extension of the control vector to the river bed and flood plain friction coefficients (ASSIM2) has recently been added into the operational flood forecasting chain and has shown very good results. The details for the ASSIM implementation in the framework of operational flood forecasting are given in Sect. 4.

4. Operational implementation at SPC SAMA

The SPC SAMA transfers a vigilance map to SCHAPI twice a day at 8:45 a.m and 2:45 p.m so that the national vigilance map can be issued at 10:00 a.m and 4:00 p.m. The real-time forecast operational chain for the Marne Amont Global (MAG) hydraulic model using DA from the ASSIM1+ASSIM2 previsouly described approach is presented in Figure 9 and

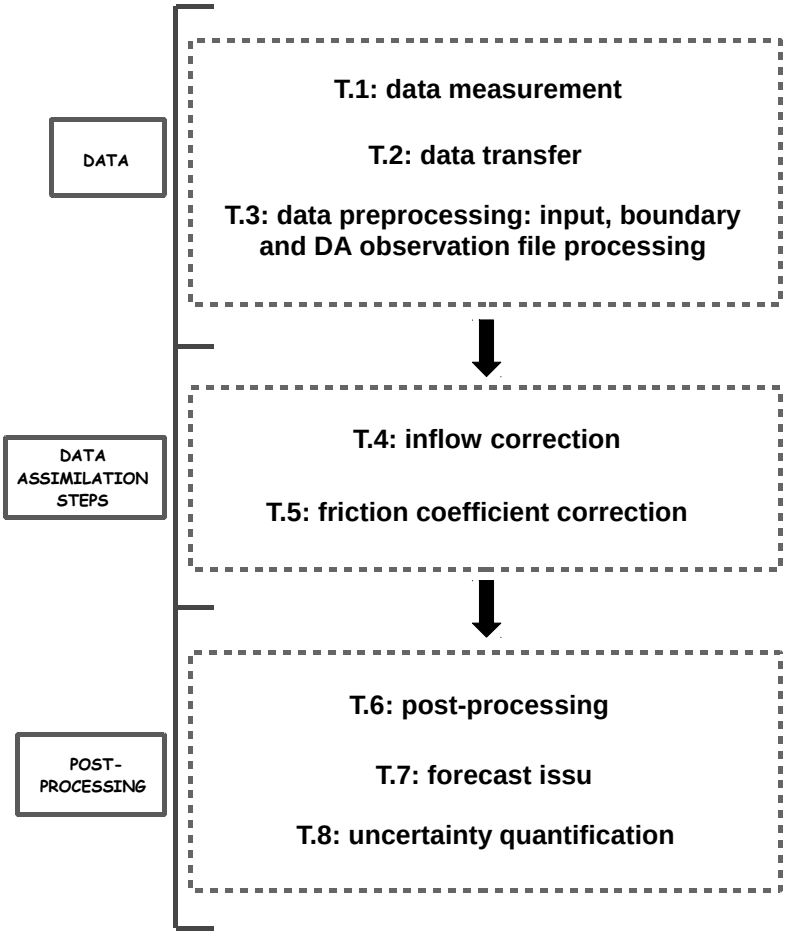

Figure 9: Operational organigram for DA applied to the Marne Amont forecast model divided in eight tasks.

is broken down in three modules. This chain should be computationally efficient to allow for the use of recently acquired data while providing informed forecasts.

The first module, named DATA, is composed of three tasks. In task 1, in-situ measurement of water levels are made at approximately 50 observing stations with automatic instruments over the SAMA catchment. In task 2, these data are gathered at SPC through telephone network four times a day, up to hourly during a flood event. The quality of these data is controlled and, when not observed, discharge data are computed using a local rating curve. Task 3 consists in pre-processing the observed data to provide to input files for the hydraulic model. Depending on the average flow conditions in the network, an initialisation

file for the MAG model is chosen amongst a pre-computed input files data base for low, medium and high flow. Using data from the upstream observing stations, 9 files for the boundary conditions for the hydraulic network are automatically generated for each analysis time T over [T-54h,T], with a constant extension over [T,T+21h] (maximum lead time at Chamouilley). Water level and discharge observations files are automatically generated at the assimilation station of Condes, Mussey, Joinville, Chamouilley and Saucourt over [T-6h,T] for the assimilation analysis.

The second module, DA STEPS, gathers two tasks that launch the DA steps. Task 4 represents the ASSIM1 step of the DA procedure : observed discharges are assimilated at Condes, Mussey, Chamouilley and Saucourt to correct upstream and lateral inflows. The corrected forcing files are stored for use in task 5.Task 5 represents the ASSIM2 step of the DA procedure: observed water levels at Joinville are assimilated to correct the local friction coefficients. The improved bathymetry from BATHY in the neighboring of Mussey is used in the operational model MAG, thus improving the model $H - Q$ relation locally. As a consequence, there is no need to assimilate observed water level at Mussey.

The third module is dedicated to POST-PROCESSING of the analysis. The REF and ASSM1+ASSIM2 result files are exported in task 6 to a server for post-treatement using a supervision software that provides the forecaster with an integrated hydrological situation of the catchment. In task 7, based on the provided forecast and his expertise, the forecaster is finally able to characterize the flood risk within the risk-color panel.

In the third module, this information is then published by SCHAPI on the vigicrues web site and communicated to the Civil Services. Task 8 is dedicated to quantifying the uncertainty (UQ) related to the forecasted water level. Considering a gaussian-shaped error on the controled friction coefficients and forcing corrective parameters, the analysis error is used to define a so-called analysis interval between the 10th and the 90th quantiles. Integrating a limited number of additional model runs for these interval limits thus provides an on-line envelope for forecasted water level. An additional information on the forecasted water level is given by a set of abacus that are set up off line. The difference between the simulated and observed water level for the eight validation flood events are computed and

classified in quantiles for each forecast lead time. The median, 10th and 90th quantiles are identified and used in the operational chain to provide an uncertainty range for the analysed water level. The computational cost of the full chain is about 4 minutes on a mono processor work station. Both uncertainty ranges are represented in Figure 10 for the Decembre 2011 event at Joinville. On December 18th at 1 p.m, the REF model (dashed line) overestimates the observed water level (black dots) reaching the orange threshold. ASSIM1+ASSIM2 analysis (squared solid line) provides a water level that is below the threshold with an uncertainty range that remains below (or extremely close to) the orange threshold for both off-line and on-line UQ methods (grey and hatched envelopes).

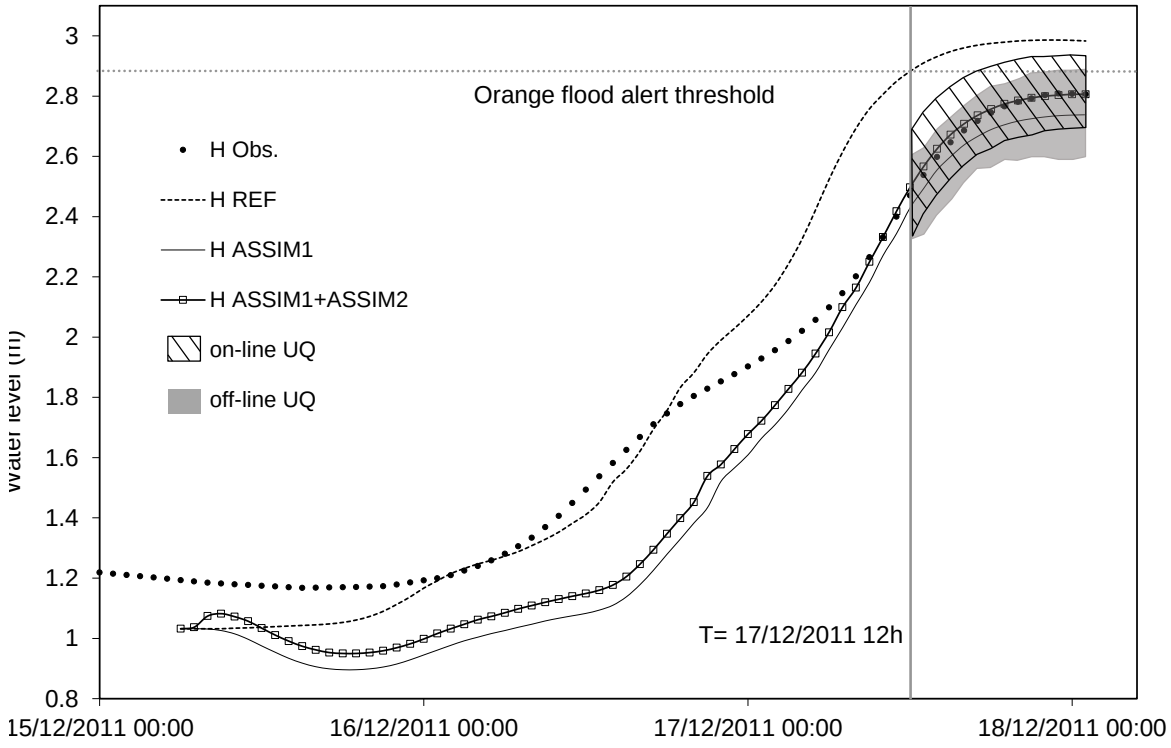

Figure 10: Observed water level (black dots) and forecasts for REF (dashed line), background from ASSIM1 (thin solid line) and ASSIM1+ASSIM2 (squared solid line) at Joinville for the December 2011 flood event. Uncertainties computed with on-line and off-line methods are represented with grey-colored and hatched areas.

5. Conclusion

This paper addressed the errors in the water level-discharge relation of a 1D hydraulic model (MASCARET) in order to improve the forecasted water level state in the context of operational flood forecasting; this water level is used to generate a colored flood risk map at the French national level by SCHAPI. This improvement is obtained over the Marne catchment through the integration of additional bathymetry data and water level measurements. In this work, it was first exhibited that a local densification of the description of the river bed geometry leads to an improved water level simulation compared to the reference model issued from a batch calibration process. The corrected bathymetry is used in the model to build a rating curve that is found to be in good agreement with recent high flow gauging. In operational context, this new rating curve is used to provide discharge from hourly observed water level. At high flow, both water level and discharge are slightly underestimated. The model can thus be improved by sequentially correcting the upstream and lateral inputs to the models that are known to be imperfect approximation of hydrologic flows for the hydraulic network. In an alternative strategy, it was assumed that no additional bathymetry measurement could be made and that the water level-discharge relation was improved by sequentially correcting the river bed and flood plain friction coefficients. An extended Kalman filter (EKF) algorithm assimilates first hourly discharge observations to correct inflows, then water level observations are assimilated to locally correct the friction coefficients. This sequential approach provides a time-dependent correction of the friction coefficients that accounts for errors in the friction and bathymetry description that vary along with the flow as water level reaches different portions of the described geometry. A sensitivity study showed that the model response is weakly nonlinear with respect to the friction coefficients when the perturbation in the friction coefficient values remains bounded. Both methods were applied in operational context and the Nash-Sutcliffe coefficient for both water level and discharge was computed over eight validation flood events and greatly improved compared to the reference model.

At SPC SAMA, both approaches are currently used for operational flood forecasting. The

densified bathymetry description is used in the neighboring of the Mussey observing station and water level data are assimilated to improve the water level-discharge relation in the model in the neighboring of the Joinville observing station. An estimation of the analyzed water level is also provided based on off-line abacus computed from a set of comparisons between the model and the observations over past events. The two-step EKF-based data assimilation approach also provides an error analysis variance for the river bed and flood plain friction coefficients that are used to describe a confidence interval for the forecasted water level.

In further work, the control vector should be extended to bathymetry profiles using parametric correction, in order to limit the equifinality issue as well as the size of the control vector to remain compatible with operational framework. The friction coefficients correction will be extended to long-distance reaches; it should allow for a temporal adjustment over a flood event and thereby for a significant improvement of the forecast lead time. A spatially and time varying correction of the hydraulic parameters is the next challenge in line. For that purpose, the use of spatially distributed data such as remote sensing data should be investigated. High-resolution data with global coverage such as those from the upcoming SWOT (Surface Water and Ocean Topography) mission will provide a new way to fully describe the river hydrodynamics. Operational flood forecasting centers should thus be prepared to make the most of the combination of remote sensing and in-situ data to design future vigilance products.

Acknowledgment

The financial support provided by SCHAPI, DREAL and SPC SAMA was greatly appreciated. The authors also gratefully acknowledge Florent Duchaine, Thierry Morel, Anthony Thévenin (CERFACS) for support on OpenPALM and on the Parasol functionality.

Bibliography

[1] K.M. Andreadis, E.A. Clark, D.P. Lettenmaier, and D.E. Alsdorf. Prospects for river discharge and depth estimation through assimilation of swath-altimetry into a raster-based hydrodynamics model.

566 *Geophysical Research Letters*, 34:L10403, 2007.
567 [2] G. Aronica, B. Hankin, and K. Beven. Uncertainty and equifinality in calibrating distributed roughness
568 coefficients in a flood propagation model with limited data. *Advance Water Resources*, 22:349–365, 1998.
569 [3] M. Audinet and H. André. *Hydrométrie appliquée aux cours d'eau.* Collection EDF-DER no. 91, 1995.
570 [4] H. Bessiere, H. Roux, and D. Dartus. Data assimilation and distributed flash flood modeling. In
571 *Hydrology Workshop*, 2007.
572 [5] K. Beven and J. Freer. A dynamic topmodel. *Hydrological Processes*, 15:1993–2011, 2001.
573 [6] S. Buis, A. Piacentini, and D. Déclat. Palm: a computational framework for assembling high perfor-
574 mance computing applications. *Concurrency and Computation: Practise and Experience*, 18(2):247–
575 262, 2006.
576 [7] CEMAGREF. *L'extrapolation des courbes de tarage en hydrométrie.* Note technique no. 10, 1981.
577 [8] A.P.J. de Roo, B. Gouweleeuw, and J. Thielen. Development of a european flood forecasting system.
578 *International Journal River Bassin Management*, 1:49–59, 2003.
579 [9] C.M. DeChant and H. Moradkhani. Improving the characterization of initial condition for ensemble
580 streamflow prediction using data assimilation. *Hydrology and Earth System Sciences*, 15:3399–3410,
581 2011.
582 [10] C.M. DeChant and H. Moradkhani. Radiance data assimilation for operational snow and streamflow
583 forecasting. *Advances in Water Resources*, 34:351–364, 2011.
584 [11] M. Durand, K.M. Andreadis, D.E. Alsdorf, D.P. Lettenmaier, D. Molller, and M. Wilson. Estimation
585 of bathymetric depth and slope from data assimilation of swath altimetry into a hydrodynamic model.
586 *Geophysical Research Letters*, 35:L20401, 2008.
587 [12] N. Goutal and F. Maurel. A finite volume solver for 1d shallow water equations applied to an actual
588 river. *International Journal for Numerical Methods in Fluids*, 38(2):1–19, 2002.
589 [13] J. Habert, S. Ricci, E. Le Pape, O. Thual, N. Goutal, F. Zaoui, and R. Ata. Towards real-time flood
590 forecasting in hydraulics: Merits of in situ discharge and water level data assimilation for the modeling
591 of the marne catchment in france. In *Advances in Hydroinformatics - SIMHYDRO 2012 - New Frontiers*
592 *of Simulation Séries : Springer Hydrogeolog Conference Simhydro*, 2012.
593 [14] J. Hartnack, H. Madsen, and J. Tornfeldt Sorensen. Data assimilation in a combined 1d-2d flood
594 model. *Proceedings of the International Conference Innovation, Advances and Implementation of Flood*
595 *Forecasting Technology of Tromso*, pages 1–8, 2005.
596 [15] Nelly Jean-Baptiste. *Assimilation de données pour l'estimation de l'état hydraulique d'un aménagement*
597 *hydroéléctrique du Rhône équipé de la commande prédictive.* PhD thesis, Université de Toulouse, 2011.
598 [16] E. Jeremiah, S. Sisson, L. Marshall, R. Mehotra, and A. Sharma. Bayesian calibration and uncertainty
599 analysis of hydrological models: a comparaison of adaptive metropolis and sequential monte carlo

samplers. *Water Resources Research*, 47:W07547, 2011.

[17] E. Kalnay. *Atmospheric modeling, data assimilation and predictability.* Cambridge University Press, 2003.

[18] J. Kirchner. Getting the right answers for the right reasons: Linking measurements, analyses, and models to advance the science of hydrology. *Water Resources Research*, 42:W03S04, 2006.

[19] Y. Liu and H.V. Gupta. Uncertainty in hydrologic modeling: Toward an integrated data assimilation framework. *Journal of Hydrology*, 397:211–224, 2011.

[20] H. Madsen and C. Skotner. Adaptative state updating in real-time river flow forecasting – a combined filtering and error forecasting procedure. *Journal of Hydrology*, 308:302–312, 2005.

[21] P. Matgen, M. Montanari, R. Hostache, L. Pfister, L. Hoffmann, D. Plaza, V.R.N. Pauwels, G.J.M. De Lannoy, R. De Keyser, and H.H.G. Savenije. Towards the sequential assimilation of sar-derived water stages into hydraulic models using the particle filter: proof and concept. *Hydrology and Earth System Sciences*, 14:1773–1785, 2010.

[22] MEDDE. Tableau des événements naturels dommageables survenus en france de 1900 a 2010. *prim.net*, aout 2011.

[23] H. Moradkhani, K. Hsu, H. Gupta, and S. Sorooshian. Uncertainty assessment of hydrologic model states and parameters: sequential data assimilation using the particle filter. *Water Resources Research*, 41:W05012, 2005.

[24] H. Moradkhani, S. Sorooshian, H. Gupta, and P. Houser. Dual state-parameter estimation of hydrological models using ensemble kalman filter. *Advances in Water Resources*, 28:135–147, 2005.

[25] J.C. Neal, P.M. Atkinson, and C.W. Hutton. Flood inundation model updating using an ensemble kalman filter and spatially distributed measurements. *Journal of Hydrology*, 336:401–415, 2007.

[26] J.C. Neal, G. Schumann, P. Bates, W. Buytaert, P. Matgen, and F. Pappenberger. A data assimilation approach to discharge estimation from space. *Hydrological Processes*, 23:3641–3649, 2009.

[27] M.A. Parrish, H. Moradkhani, and C.M. DeChant. Toward reduction of model uncertainty: Integration of bayesian model averaging and data assimilation. *Water Resources Research*, 48:W03519, 2012.

[28] W. Peters, J.B. Miller, J. Whitaker, A.S. Denning, A. Hirsch, M.C. Krol, D. Zupanski, L. Bruhwiler, and P.P. Tans. An ensemble data assimilation system to estimate co2 surface fluxes from atmospheric trace gas observations. *Journal of Geophysical Research*, 110:D24304, 2005.

[29] G. Petron, C. Granier, B. Khattatov adn J.F. Lamarque, V. Yudin, J.F. Muller, and J. Gille. Inverse modeling of carbon monoxide surface emissions using climate monitoring and diagnostics laboratory network observations. *Journal of Geophysical Research*, 107(D24):4761, 2002.

[30] B. Renard, D. Kavetski, G. Kuczera, M. Thyer, and S.W. Franks. Understanding predictive uncertainty in hydrologic modelling: The challenge of identifying input and structural errors. *Water Resources*

Research, 46:W05521, 2010.

[31] S. Ricci, A. Piacentini, O. Thual, E. Le Pape, and G. Jonville. Correction of upstream flow and hydraulic state with data assimilation in the context of flood forecasting. *Hydrology and Earth System Sciences*, 7:1–55, 2011.

[32] M.C. Rochoux, S. Ricci, D. Lucor, B. Cuenot, and A. Trouvé. Towards predictive data-driven simulations of wildfire spread. part i: Reduced-cost ensemble kalman filter based on a polynomial chaos surrogate model for parameter estimation. *Natural Hazards and Earth System Sciences*, 2(5):3289–3349, 2014.

[33] J.R. Stedinger, R.M. Vogel, S.U. Lee, and R. Batchelder. Appraisal of the generalized likelihood uncertainty estimation (glue) method. *Water Resources Research*, 44:W00B06, 2008.

[34] J.M. Van der Knijff, J. Younis, and A.P.J. de Roo. Lisflood: a gis-based distributed model for river-basin scale water balance and flood simulation. *International Journal of Geographical Information Science*, 24(2):189–212, 2010.

[35] J.A. Vrugt, C.G.H. Diks, H.V. Gupta, W. Bouten, and J.M. Verstraten. Improved treatment of uncertainty in hydrologic modeling: Combining the strengths of global optimization and data assimilation. *Water Resources Research*, 41:W01017, 2005.

[36] J.A. Vrugt, C.J.F. ter Braak, M.P. Clark, J.M. Hyman, and B.A. Robinson. Treatment of input uncertainty in hydrologic modeling: Doing hydrology backward with markov chain monte carlo simulation. *Water Resources Research*, 44(12):W00B09, 2008.

[37] A.H. Weerts, H.C. Winsemius, and J.S. Verkade. Estimation of predictive hydrological uncertainty using quantile regression: examples from the national flood forecasting system. *Hydrology and Earth Systeme Sciences*, 15:255–265, 2011.

[38] M. Werner, M. Cranston, T. Harrison, D. Withfield, and J. Schellekens. Recent developments in operational flood forecasting in england, wales and scotland. *Royal Meteorology Society*, 16:13–22, 2009.

This paper presents a data-driven hydrodynamic simulator based on the 1-D hydraulic solver dedicated to flood forecasting with lead time of an hour up to 24 hours. The goal of the study is to reduce uncertainties in the hydraulic model and thus provide more reliable simulation and forecast in real time for operational use by the national hydrometeorological flood forecasting center in France. Previous studies have shown that sequential assimilation of water level or discharge data allows to adjust the inflows to the hydraulic network resulting in a significant improvement of the discharge while leaving the water level state imperfect. Two strategies are proposed here to improve the water level-discharge relation in the model. At first, a modeling strategy consists in improving the description of the river bed geometry using topographic and bathymetric measurements. Secondly, an inverse modeling strategy proposes to locally correct friction coefficients in the river bed and the flood plain through the assimilation of in-situ water level measurements. This approach is based on an Extended Kalman filter algorithm that sequentially assimilates data to infer the upstream and lateral inflows at first and then the friction coefficients. It provides a time varying correction of the hydrological boundary conditions and hydraulic parameters.

The merits of both strategies are demonstrated on the Marne catchment in France for eight validation flood events and the January 2004 flood event is used as an illustrative example throughout the paper. The Nash-Sutcliffe criterion for water level is improved from 0.135 to 0.832 for a 12-hour forecast lead time with the data assimilation strategy. These developments have been implemented at the SAMA SPC (local flood forecasting service in the Haute-Marne French department) and used for operational forecast since 2013. They were shown to provide an efficient tool for evaluating flood risk and to improve the flood early warning system. Complementary with the deterministic forecast of the hydraulic state, an estimation of an uncertainty range is given relying on off-line and on-line diagnosis. The possibilities to further extend the control vector while limiting the computational cost and equifinality problem are finally discussed.